Conversion of lignocellulose into biochar and furfural through boron complexation and esterification reactions

Jingfa Zhang [a,b], Ahmed Koubaa[b], Dan Xing[b], Haigang Wang[a*], Yonggui Wang[a], Wanyu Liu[a], Zhijun Zhang[a], XiangMing Wang[c] and Qingwen Wang[d]

[a] Key Laboratory of Bio-based Materials Science and Technology (Ministry of Education), Northeast Forestry University, Harbin 150040, P. R. China.

[b] Université du Québec en Abitibi-Témiscamingue, Rouyn-Noranda, J9X 5E4, Québec, Canada.

[c] New Construction Materials, FPInnovations, Québec, G1V 4C7, Québec, Canada.

[d] College of Materials and Energy, South China Agricultural University, Guangzhou 510642, P.R. China.

Corresponding author: hgwang@nefu.edu.cn (Haigang Wang)

Abstract

The aim of this work was to study the conversion of lignocellulose into biochar and furfural through boron complexation and esterification reaction. Boric acid was used to modify lignocellulose to obtain a high biochar yield boron-lignocellulosic material through complexation and esterification reactions. Furthermore, clean furfural was obtained as the gas products of boron-lignocellulosic materials pyrolysis. The structures of the boron-lignocellulosic materials were characterized, and their compound principle was revealed. Boric acid treatments increased the initial thermal degradation temperature of lignocellulose and promoted the formation of biochar and furfural. The biochar yield rate increased by 135.7% from 18.6 to 42.9% at 600 ℃ after 5% boric acid solution treatment. Compared with pure lignocellulose, cleaner and higher quantities of furfural were obtained from boron-lignocellulose pyrolysis. Finally, the possible chemical decomposition pathways of boron-

lignocellulosic materials were identified. This study provides a new perspective on the thermochemical conversion of lignocellulose to furfural and biochar.

Keywords: lignocellulose; boric acid; thermal conversion; biochar; furfural

1. Introduction

Lignocellulose, which is primarily composed of cellulose, hemicellulose and lignin, has long been a favored material by researchers. Interestingly, new uses and functions for lignocellulosic-based materials are proposed on a daily basis (Herou et al., 2019; Li et al., 2018a; Li et al., 2019; Wang et al., 2019). Recently, studies on lignocellulose/polymer composites, biochar, biomass-derived chemicals and bio-pyrolysis oil have received considerable interest from both academia and industry (Ahmed et al., 2019; Dai et al., 2019; Lu et al., 2019). Thus, there is a need to enhance the understanding of the thermal properties and decomposition of lignocellulose. Chemical modification is a common method for improving the performance of lignocellulosic materials. The effects of chemical modification on the mechanical properties, optics, thermal conversion, fire retardancy and dimensional stability of lignocellulose have been investigated extensively (Berglund & Burgert, 2018; He et al., 2018; Li et al., 2018b). However, the effects of boric acid on the structure and thermal properties of lignocellulosic materials and its chemical mechanisms remains unclear.

Boric acid has been used as a preservative and flame retardant for a long time in the lignocellulosic materials industry. Boric acid can also increase the thermal degradation temperature of lignocellulosic materials because that it is believed to change into a layer of

43 B_2O_3 film that isolates oxygen and heat (Uner et al., 2016), which is also widely believed to
44 be the mechanism by which boric acid induces flame retardancy. However, Wang *et al.*(Wang
45 et al., 2004) argue that boric acid complexes with lignocellulose to produce hydrogen ions,
46 which can catalyze the conversion of lignocellulose into biochar. Furthermore, Wicklein *et al.*
47 (Wicklein et al., 2016) found that nanocellulose can complex with boric acid under alkaline
48 conditions to achieve flame retardancy. The effect of boric acid on the thermal performance
49 of lignocellulosic materials and its retardancy mechanism remains uncertain. Boric acid has
50 also been used to improve the thermal stability of sugars and phenolic resins through
51 esterification or complexation reactions (Ricardo et al., 2004; Wang et al., 2014). It is worth
52 noting that boric acid can react with polyhydroxy compounds, such as polyols, carbohydrates,
53 proteins and vitamins (Peters, 2014). Various bonding mechanisms between boric acid and
54 polyhydroxy compounds exist, including monoesters and cyclic diester structures with
55 negatively charged tetrahedral boron anions (Miyazaki et al., 2013).

56 Most studies have primarily focused on the effect of boric acid as a fire retardant for
57 lignocellulose combustion. However, there is a comparative lack of information related to the
58 effect of boric acid modification on the thermal conversion of lignocellulose and their
59 pyrolysis pathway. Here, effects of boric acid modification on lignocellulose thermal
60 conversion behaviors were explore. Specifically, lignocellulose was treated with boric acid
61 solutions at different concentrations. The treated samples were then characterized to identify
62 the chemical reaction mechanism between boric acid and lignocellulose. Furthermore, the
63 authors explored the effect of boric acid on the thermal conversion behavior of lignocellulosic

materials and elucidated the mechanism of thermal decomposition of borated lignocellulosic materials.

2. Materials and methods

2.1 Materials

Lignocellulose (poplar-wood fiber) (Harbin, China) was purchased from the market and ground into wood flour (40~80 mesh). Holocellulose was prepared according to Jayme (Jayme, 1942). Analytical reagent grade lignin, mannitol, glycerin, microcrystalline cellulose and boric acid were obtained from Sigma-Aldrich.

2.2 Preparation of boron-lignocellulose hybrid materials (borated lignocellulose)

A 200 mL solution (5% by weight) of boric acid was prepared by dissolving the acid in distilled water in a 500-mL glass container at 50 ℃ under vigorous magnetic stirring. Lignocellulose was subsequently added to this solution at ambient temperature, allowed to stand for 2 hours and then filtered and dried at 105 ℃ for 24 h. The same treatment was used for holocellulose, MCC and lignin.

Glycerin (0.05 M) and boric acid (0.05 M) were dissolved in 100 mL of deionized water in a 200-ml glass container at 50 ℃ under vigorous magnetic stirring. The solution was then concentrated using an oven at 105 ℃ for 24 h. The mixture was further dehydrated using a vacuum drying oven at 50 ℃ for 24 h. Mannitol and glucose were treated using the same procedure.

2.3 Characterization

84 2.3.1 Chemical structure of borated lignocellulose

85 Fourier-transform infrared (FTIR) spectra were recorded in the range of 4000–600 cm^{-1}
86 at a resolution of 4 cm^{-1} with an average of 32 scans, employing a Nicolet 6700 with ATR
87 module (Thermo Fisher Scientific Co., Ltd., USA). X-ray photoelectron spectroscopic (XPS)
88 measurements were obtained using a K-alpha X-ray photoelectron spectrometer (Thermo
89 Fisher Scientific Co., Ltd. USA). The spectrum energy scale was calibrated referencing the
90 C1s peak of adventitious aliphatic carbon (284.5 eV).

91 2.3.2 X-ray diffraction (XRD) analysis

92 XRD patterns of untreated lignocellulosic materials and samples modified with different
93 concentrations of boric acid were measured using an X-ray diffractometer (D/max 2200,
94 Rigaku, Japan) equipped with Ni-filtered Cu Kα radiation (λ=1.5406 A) at 40 kV and 30 mA.
95 The scan range of 2θ was set to 5–40° with a speed of 1° min^{-1}. The crystallinity index (*CrI*)
96 of samples was calculated according to the Segal method (Segal et al., 1959):

97 $$CrI = \frac{I_{002} - I_{am}}{I_{002}} \quad (1)$$

98 where *CrI* refers to relative crystallinity, I_{002} is the maximum intensity of the 002 lattice
99 (2θ=22.8°) and I_{am} is the intensity of the valley between the 002 and 101 lattice peaks
100 (2θ=18.0°), indicating the scattering intensity of the amorphous background diffraction.

101 2.3.3 Thermogravimetric analysis

The thermogravimetric analysis (TGA) was conducted using a TGA-400 (Perkin-Elmer, USA). The samples were heated from room temperature to 600 ℃ at a heating rate of 10 ℃·min^{-1} under a nitrogen atmosphere, with a purge gas flow of 40 ml·min^{-1}.

2.3.4 Color analysis

The color of the lignocellulose was characterized using a CR-400 chroma meter (Konica Minolta, Japan) with a CIE Lab system. The color values L^*, a^* and b^* in the color space of CIE $L^*a^*b^*$, were recorded for each specimen. Color values were recorded for five parallel samples, then averaged. The ΔL^*, Δa^* and Δb^* were calculated using lignocellulose dried at 105 ℃ as a reference (e.g. $\Delta L^* = L^*_1 - L^*_{control}$). The color difference ΔE^*, which expresses the total color change, was calculated according to Eq. (2):

$$\Delta E^* = \sqrt{(\Delta L^{*2} + \Delta a^{*2} + \Delta b^{*2})} \quad (2)$$

2.3.5 Energy dispersive spectrometer (EDS)

The surface elements of lignocellulose were analyzed using an energy dispersive spectrometer (X-MAX 20 mm^2, Oxford Instrument, UK). Before the test, a poplar woodblock (2 × 2 mm) was immersed in a 5% boric acid solution for 24 h and then sliced by a microtome (HM325, Thermo Fisher Scientific, USA). These slices were then dried and coated with gold powder.

2.3.6 Pyrolysis coupled Gas Chromatography-Mass Spectrometry (Py-GC/MS)

Fast pyrolysis experiments were performed using a CDS5200HP-R pyrolyzer directly connected to an Agilent 6890N gas chromatograph (GC) which was coupled to an Agilent 5973i mass spectrometer (MS) (Agilent Technologies, Palo Alto, USA). The MS was

operated in electron impact mode at 70 eV over the m/z range from 40 to 500 amu. Samples of 0.5 mg were held with loose quartz wool packing in a quartz sample tube. All pyrolysis tests were carried out at 300 ℃ for 15 s with a heating rate of 20 ℃·ms^{-1} using a platinum coil probe. The pyrolysis chamber was purged with helium carrier gas at a flow rate of 20 mL ·min^{-1}. Gas chromatography-mass spectrometry was applied to separate and identify the pyrolysis products. The chromatographic signals were identified by comparing the experimental mass spectrum to the mass spectrum library provided by the program.

3. Results and Discussion

3.1 Chemical structure of borated lignocellulosic materials

It is well known that boric acid can react with glycerin and mannitol, forming complexes and borated esters (Miyazaki et al., 2013). FTIR and XPS spectra of the borated glycerin, borated mannitol and borated lignocellulosic materials were obtained and compared to explore the reaction between boric acid and lignocellulosic materials. Compared to pure lignocellulose, new intense signals at 3200, 1380, 1340, 1280, 1200, 940 and 810 cm^{-1} appeared in the FTIR spectrum of the borated lignocellulose. The characteristic peak at 3200 cm^{-1} can be attributed to the stretching vibrations of hydroxyl groups in boric acid (Xia et al., 1995). The bands at 1380 and 1340 cm^{-1} belong to the bridge stretching vibration of B-O-B and B-O-C bonds, respectively (Wang et al., 2015). The band at 1280 cm^{-1} corresponded to the stretching vibrations of the B-O bonds of "boroxol rings" (Feng et al., 2011). It revealed that the self-association of boric acid, a special type of interaction, occured in this system. This observation was consistent with the NMR result obtained by Coddington *et*

144 *al.*(Coddington & Taylor, 1989), which demonstrated the presence of 'boroxol rings' in boric
145 acid-polyol compounds. The band at 1200 cm^{-1} can be attributed to the in-plane bending
146 vibration of the B-O bond (Xia et al., 1995). The bands at 940 cm^{-1} and 850 cm^{-1} were
147 ascribed to the valence vibrations of B-O in a BO_4^- tetrahedra (Xia et al., 1995). The
148 characteristic bands of tricoordinate and tetrahedra boron were also observed in the FTIR
149 spectra of borated glycerin and mannitol compounds. These observations indicated that boric
150 acid could react with lignocellulose through esterification and complexation reactions.

151 In addition, the characteristic bands of borate esters and borate complexes were present
152 in the FTIR spectra of borated holocellulose and borated lignin. Whereas there were few
153 differences between the FTIR spectra of micro-cellulose (MCC) and borated MCC. With its
154 robust crystalline structure, MCC was hardly soaked and reacted with boric acid. Compared
155 with MCC, nanocellulose in lignocellulose has more free hydroxyl groups, which is favorable
156 for the complexation reaction. Indeed, a previous study has shown that a cross-linking of
157 boric acid and nanocellulose forms under alkaline conditions (Wicklein et al., 2016). Overall,
158 boric acid reacted with the amorphous region of cellulose in lignocellulosic materials.

159 The high-resolution B 1s XPS spectrum of borated lignocellulose can be deconvoluted
160 into three peaks of B1 at 194.3 eV, B2 at 193.5 eV and B3 at 192.8 eV. The peak at 194.3 is
161 attributed to the B–OH, while the other two components, B2 at 193.5 eV and B3 at 192.8 eV,
162 are related to the B–O–B and B–O–C bonds, respectively (Wang et al., 2015). This result was
163 in highly consistent with the FTIR results, indicating that boric acid reacted with
164 lignocellulose. These three peaks were also observed in the high-resolution B 1s XPS spectra

of glycerin-BA, mannitol-BA, holocellulose-BA and lignin-BA. However, the B-O-C bond was not observed in the B 1s XPS spectrum of borated MCC, indicating that the complexation or esterification reaction of boric acid and MCC did not occur. Although evidence for the reaction of boric acid and MCC was absent, it is believed that boric acid appeared capable of reacting with the amorphous cellulose in lignocellulose according to the FTIR and XPS results for lignocellulose and holocellulose. The results from the XPS were in good agreement with the FTIR results, which indicated that a chemical reaction between boric acid and lignocellulosic materials occurred during boric acid treatment.

The effects of boric acid on the crystallization of lignocellulose were analyzed by X-ray diffraction. The crystallinity (*CrI*) of lignocellulose treated with boric acid decreased compared to untreated lignocellulose. *CrI* decreased with an increase in the concentration of the boric acid solution, from 51.4% in untreated lignocellulose to 41.4% in lignocellulose + 5% BA. The decrease in crystallinity resulting from lignocellulose swelling was caused by the boric acid solution. Boric acid attacked amorphous regions of cellulose in a manner similar to water, forcing the microfibrils apart and leading to damage of the crystalline cellulose. However, the intermolecular and intramolecular hydrogen bonds within the cellulose crystalline region disintegrated and were replaced by borate bonds during the treatment. Boric acid treatment not only reduced the *CrI* of lignocellulose but also influenced its crystalline form. A diffraction shoulder peak at $2\theta = 20.60^{\circ}$ appeared when the boric acid solution concentration was greater than 3 wt %. This peak can be attributed to the $10\bar{1}$ diffraction crystal face of cellulose II (El Oudiani et al., 2011). This result indicates that the

boric acid treatment partially changed the crystal form of cellulose, from cellulose I to cellulose II. Compared to cellulose I, cellulose II is more beneficial to the formation of biochar by pyrolysis (Kolpak & Blackwell, 1976), leading to robust fire retardancy for boric acid treated lignocellulosic materials. However, the strength of cellulose II is lower than that of cellulose I which is caused by the smaller molecular weight of cellulose II compared to cellulose I (El Oudiani et al., 2011). The decrease in molecular weight may also lead to a decrease in *CrI*. Moreover, a diffraction peak of boric acid appeared in the XRD spectrum of the borated lignocellulose when the concentration of boric acid was above 3 wt%. This result showed that there was unreacted boric acid remaining in lignocellulose-BA. Furthermore, boron oxide films on the lignocellulose surface were revealed by the microscopic image. The EDS results showed that the distribution of the boron element was the same as that of carbon and oxygen elements, indicating the boron was evenly distributed in the cell wall. Residual boric acid increased with the concentration of the boric acid solution. The weight gain rate (WPG) of borated lignocellulose increased with the boric acid solution concentration increasing. A maximum increase of WPG was obtained in lignocellulose + 5% BA, and it was 25.9%. However, the WPG decreased obviously after leaching using distilled water. This observation revealed that boron-lignocellulose had poor resistance to mass loss during leaching.

Hence, boric acid not only reacted with lignocellulose through esterification and complexation but also altered its crystalline behavior. The chemical structure of borated lignocellulose was obtained after lignocellulose was treated by boric acid solutions.

Additionally, the cross-linking degree of lignocellulose increased, which resulted from the link of B–O–B and B-O-C bonds (Wicklein et al., 2016).

3.2 Thermal degradation of the borated lignocellulosic materials

The thermal degradation of untreated lignocellulose took place in two steps, the degradation of hemicellulose (220-320 ℃) and cellulose (320-400 ℃), while lignin degradation accompanied the entire process (Fig. 1a). The boric acid treatment altered the thermal degradation behavior of the lignocellulose, and the degradation process of borated lignocellulose can be divided into three stages (Figs. 1a and 2a). The dehydration of self-polymerization of boric acid and the dehydration resulting from the complexation of boric acid and hydroxyl groups were the main contributors to the weight loss in the first stage. The second stage involved the decomposition of hemicellulose and cellulose. The pyrolysis peaks of cellulose and hemicellulose were combined into one peak because the boric acid treatment increased the hemicellulose degradation temperature. Furthermore, it is worth noting that the initial degradation temperature of hemicellulose increased. Lignocellulose degradation mainly occurred during the second stage. The last stage involved a further cracking of the borated polysaccharide and the associated rupture of the cyclic B-O-C bonds, which can be attributed to esterification and complex formation between the boron and hydroxyl groups. Compared to untreated lignocellulose, the temperature at 20% weight loss ($T_{20\%}$) increased, whereas the temperature at 5% weight loss ($T_{5\%}$) decreased for borated lignocellulose. In addition, the maximum degradation rate of lignocellulose decreased following boric acid treatment when the concentration of the boric acid solution was greater than 3 wt% (Fig. 2a).

The residual biochar yield, which is one of the most important indicators of thermal stability, was higher for borated lignocellulose than for untreated lignocellulose. These results revealed that boric acid treatment improved the thermal stability of lignocellulose. However, the temperature at the maximum degradation rate (T_{max}) of the borated lignocellulose decreased compared to untreated lignocellulose. This finding can be explained by the fact that boric acid decreased the crystallinity of lignocellulose and partially changes its crystalline form.

The effects of boric acid on the thermal degradation behavior of holocellulose and MCC were similar to that of lignocellulose (Figs. 1b and c). However, the degradation temperature of holocellulose was lower than that of lignocellulose because of the presence of lignin. Lignin increases the cross-linking of lignocellulose, leading to a higher thermal stability for lignocellulose than for holocellulose. The boric acid treatment also increased the $T_{20\%}$, and the char yield of lignin and reduced its maximum degradation rate (Figs. 1 and 2). Contrary to lignocellulose, the T_{max} of lignin increased following the boric acid treatment. Furthermore, boric acid treatment also had a positive effect on the thermal stability of glycerin and mannitol.

The boric acid treatment had no influence on the color of lignocellulose; however, it reduced the rate of blackening caused by the heat treatment. Pure lignocellulose and lignocellulose treated with a 5 wt% boric acid solution were heat-treated at 220 ° C for 2 hours using a drying furnace. For lignocellulose, the lightness (L^*), redness (a^*) and yellowness (b^*) values decreased after the heat treatment. The maximum color change (ΔE^*) was obtained after the pure heating treatment (Fig. 3). The results showed that heating made

lignocellulose become dark and reduced the red and yellow color of lignocellulose. The decrease in lightness was smaller for boric acid and heat-treated lignocellulose than for the pure heat-treated lignocellulose. The change in b^* for boric acid and heat-treated lignocellulose was negligible. The a^* of borated lignocellulose increased while that of the pure lignocellulose changed little after the heat treatment. The color analysis results revealed that boric acid improved the stability of lignocellulose, which was consistent with the TGA results.

From the TGA and color analysis results, one can ascertain that boric acid can improve the thermal stability of lignocellulosic materials and polyols, especially for the initial thermal degradation temperature and biochar yield indicator. This finding was similar to the results obtained by Uner *et al* (Uner et al., 2016). It has also been found that boric acid slowed the thermal decomposition of pentose when wood was treated with both boric acid and heating (Kartal et al., 2008). According to the aforementioned observations and previous findings (Uner et al., 2016; Wang et al., 2004; Wicklein et al., 2016), the authors proposed that the following mechanisms are involved in improving the thermal stability of lignocellulosic materials using boric acid treatment: First, boric acid reacts with the lignocellulosic materials by esterification and complexation, leading to an increase in the degree of cross-linking, which results in the improvement of the initial degradation temperature of lignocellulosic materials. Second, B–O bonds, whose bond energy (561 kJ·mol^{-1}) is greater than that of C–O bonds (384 kJ·mol^{-1}), are introduced into the lignocellulosic materials, improving the stability of their chemical structure. Third, the boric acid self-polymerization and the dehydration

reactions of B-OH with hydroxyl groups produce water and easily absorb heat, which slows the thermal degradation of the lignocellulosic materials. Fourth, boron oxide glass layers form during the thermal degradation process and isolate a part of the oxygen, leading to a high char yield. Finally, the pyrolysis chemical pathway of lignocellulosic materials changes due to the addition of boron, leading to a high biochar yield.

3.3 Change in the chemical structure of borated lignocellulosic materials during pyrolysis

3.3.1 XPS analysis of lignocellulose treated with both boric acid and heat

The change in the oxygen to carbon atomic ratio (O/C) has been used to characterize the degradation of cellulosic materials and polymers (Inari et al., 2006). In this study, the O/C ratios of the test samples were calculated using the total areas of the peaks of the oxygen and carbon components to analyze the effect of the boric acid treatment (Table 1). The O/C ratio of untreated lignocellulose decreased slightly after the heat treatment. This finding was in good agreement with those of previous studies (Kocaefe et al., 2013). This observation can be explained by the fact that the dehydration of polymers (cellulose and hemicelluloses) leads to the formation of volatile by-products and biochar during heating, resulting in decreases in carbohydrate content and increases in lignin content. The O/C ratio of untreated lignocellulose was smaller than that of borated lignocellulose due to the presence of boric acid. Contrary to untreated lignocellulose, the O/C ratio of borated lignocellulose changed little after heat treatment.

High-resolution XPS C1s spectra were also studied to evaluate the chemical structures of lignocellulose before and after the heat treatment (Fig. 4). The high-resolution C1s spectra were fitted with their decomposition into four components according to carbon-containing functional groups.(Kocaefe et al., 2013) The C_1 - C_4, corresponds to C–C and/or C–H (C_1), C–O (C_2), C=O and/or O–C–O (C_3) and O=C–O(C_4), respectively (Fig. 4). The content of the four fitted peaks was shown in Table 1 after curve fitting using Gaussian function. C_2 is considered to originate mainly from cellulose and hemicelluloses, while C_1 is primarily attributed to lignin (Peng et al., 2015). The content of C_2 decreased, whereas the content of C_1 increased for both the lignocellulose and borated lignocellulose samples following the heat treatment because of the dehydration of carbohydrates. However, changes in both C_1 and C_2 contents were less for borated lignocellulose compared with untreated lignocellulose. For borated lignocellulose, the content of C_3 increased slightly due to the oxidation reaction after heating. The XPS results indicated that boric acid slowed the alteration of the chemical structure of lignocellulose resulting from heating.

3.3.2 The pyrolysis production analysis

Similar to previous studies, the thermal decomposition of lignocellulose primarily resulted in the production of volatile organic compounds (VOC) such as carbon dioxide, 1-hydroxy-2-acetone, furfural, anhydrides, 2,5-furan carboxaldehyde, levoglucosenone, vanillin, phenol and its derivatives (E-supplement file and Table 2) (Usman et al., 2019). Boric acid had an obvious influence on lignocellulose pyrolysis by reducing the chemical composition and yield of VOCs. However, it should be noted that the relative yield of furfural obtained in

311 the presence of boron was greater than that obtained from the pyrolysis of pure
312 lignocelluloses. This finding indicates that boric acid altered the thermal decomposition
313 chemical pathway of lignocellulose. To further analyze the effect of boric acid on the thermal
314 degradation mechanism of lignocellulose, pyrolysis tests of small molecules, holocellulose,
315 glucose, MCC and lignin were also carried out. The results of Py-GC/MS for holocellulose
316 and MCC were nearly the same as that for lignocellulose.

317 Boric acid had a similar effect on the pyrolysis of lignocellulosic materials and mimic
318 compounds. Compared with pure glucose, VOC yield and composition decreased for borated
319 glucose pyrolysis. The weakening or disappearance of VOC compounds (such as
320 methylglyoxal and anhydroglucose) is usually generated by the second degradation of the
321 laevoglucose (Shen & Gu, 2009). However, the relative yield of furfural increased after boric
322 acid treatment. This finding indicated that boric acid catalyzed the production of furfural and
323 biochar instead of levoglucosan during glucose pyrolysis. In the case where boron was
324 present, the pathway in which the glucose ring ruptures and recombines to form a furan
325 structure was more common than the rearrangement of glucose to levoglucosan through
326 dehydration. Besides, boric acid may induce glucose to change to a furan structure, later
327 forming a furan borate ester that has high thermal stability (Peters, 2014; Ricardo et al., 2004).

328 **3.4 Thermal degradation mechanism for borated lignocellulosic materials**

329 The thermal decomposition mechanism of cellulose has been reported in several studies
330 (Huber et al., 2006; Patwardhan et al., 2010; Shen & Gu, 2009). Previous studies show that
331 there is competition between the primary pyrolysis reaction of depolymerization of the

glycosidic bond cleavage and glycan ring decomposition. In the presence of acids, the pyrolysis reaction pathway tends to depolymerize (Huber et al., 2006). Cellulose pyrolysis produces either levoglucosan or low molecular weight species as well as biochar. Levoglucosan, which is believed to be the predominant product of cellulose pyrolysis, is formed by the intramolecular rearrangement of the monomer units after the cleavage of the 1,4-glycosidic linkage in the cellulose polymer (Li et al., 2001). Levoglucosan then undergoes a second decomposition, producing small molecular compounds (Shen & Gu, 2009). However, boric acid changed the cellulose pyrolysis chemical pathway (E-supplement file) in this study. Specifically, the hydrogen ion released from the complexation reaction of the boric acid and hydroxyl groups catalyzed the depolymerization of cellulose. In addition, the boron complexation structure prevented the formation of levoglucosan. The B-O-C bonds replaced the hydroxy at C_6 or the carbon at another position, limiting the acetal reaction to form levoglucosan. Actually, the glucose ring opened and rearranges to form a new furan structure in the case of borate presence. In such case, most of the glucose monosaccharide became furanose, followed by dehydration to furfural and its derivatives. Furthermore, the C-O bonds of borate ester cleaved and released carbon free radicals, which reacted and led to chain propagation. Finally, two radicals collided with each other to form stable compounds, leading to the termination of the chain. For boron-cellulose, the main pyrolysis mechanism was a free-radical reaction pathway, which was conducive to biochar formation. More boron-HMF went dehydration to form char instead of yielding a 1:1 mixture of levulinic and formic acids, a pattern similar to that observed in a previous study (Shen & Gu, 2009).

353 Hemicellulose undergoes analogous reaction pathways to cellulose. However, for
354 hemicellulose pyrolysis, the predominant product is 1,4-anhydro-D-xylopyranose which is
355 formed by the cleavage of the glycosidic linkages of the xylan chain and the rearrangement of
356 the depolymerized molecules instead of levoglucose (Shen et al., 2010). It then undergoes
357 several reactions to form biochar or decompose into low molecular weight compounds
358 (Patwardhan et al., 2011; Werner et al., 2014). The impact of boric acid on the hemicellulose
359 pyrolysis mechanism is similar to that for cellulose and the detailed pathways are presented in
360 the E-supplement file. On the one hand, hemicellulose produced furfural under acid catalysis.
361 On the other hand, monosaccharide rearranged and formed into a furan structure due to the
362 presence of B-O-C bonds. Meanwhile, carbon free radicals were generated by the breaking of
363 the B-O-C linkage. Two radicals collided with each other to terminate the reaction, producing
364 stable compounds. Several reactions, including aromatization and intramolecular
365 condensation, then took place to form biochar (E-supplement file).

366 Lignin has a complex decomposition mechanism due to its complex structure. Generally,
367 a free-radical reaction pathway is believed to be one of the dominant mechanisms for the
368 degradation of lignin (Kosa et al., 2011; Zhang et al., 2019b). Free radicals are generated by
369 the cleavage of the β-O-4 lignin linkage, which can further react and lead to chain
370 propagation. However, the boric acid treatment altered the decomposition pathway and
371 reduced the VOC yields from the lignin pyrolysis (E-supplement file). On the one hand, the
372 thermal degradation temperature was improved through the increase in the degree of
373 crosslinking caused by the complexation reaction. On the other hand, the hydroxyl groups at

374 the α and γ positions, as well as the phenolic hydroxyl groups, were inhibited by the borate
375 ester. The cleavage of the link bonds, such as β-o-4', 5'-5' β'-1, produced a boron-lignin
376 monomer. The C-O bonds of the borate esters subsequently cleaved and produced free
377 radicals and phenol derivatives (E-supplement file). Finally, the chain reactions were
378 terminated by collisions of radicals, forming stable biochar covered by boron films. However,
379 the exact mechanism of lignin pyrolysis remains challenging due to its complex structure
380 (Liu et al., 2015).

381 Furthermore, it was worth noting that boric acid treatment promotes the thermal
382 conversion of polysaccharides and monosaccharides to furfural. The chemical composition of
383 the pyrolysis products was relatively simple, which also simplified product separation.
384 Furfural can then be used to produce heavy-density aviation fuel following previous literature
385 (Liu et al., 2019). However, based on the above TGA analysis, boric acid appeared to have
386 catalyzed the formation of biochar from biomass materials. The boron oxidant carried out the
387 function of electron absorption and transfer. Hence, a boric acid treatment would be
388 conducive to the use of biochar in battery and solar cells. In addition, many applications
389 using biochar, such as carbon fixation, drug delivery, environmental restoration,
390 supercapacitor electrodes and batteries have been extensively studied (Haffner-Staton et al.,
391 2016; Yu et al., 2019; Zhang et al., 2019a).

392 **Conclusions**

393 Boron-lignocellulose was fabricated using boric acid treatment through complexation
394 and esterification reactions. Multiple effects of boric acid on the thermal conversion of

lignocellulose were observed and its detailed mechanisms were revealed. Boric acid changed the crystalline form of the lignocellulose from cellulose I to cellulose II. The free radical pathway was the main mechanism of boron-lignocellulose thermal degradation, which was conducive to the formation biochar. Besides, the B-O-C bonds blocked the hydroxy group in the sugar units, promoting the production of furfural during pyrolysis. These findings promise to contribute to the production of furfural from glucose or lignocellulose.

Acknowledgments

The authors thank the financial support from the National Key Research and Development Program of China (2019YFD1101203), the Fundamental Research Funds for the Central Universities (2572018BB07), and the Canada Research Chair Program, Natural sciences and Engineering Research Council of Canada. In addition, the author Jingfa Zhang (201706600026) is supported by the China Scholarship Council.

Appendix A. Supplementary data

E-supplementary data for this work can be found in e-version of this paper online.

References

1. Ahmed, M., Okoye, P., Hummadi, E., Hameed, B. 2019. High-performance porous biochar from the pyrolysis of natural and renewable seaweed (Gelidiella acerosa) and its application for the adsorption of methylene blue. *Bioresource technology*, **278**, 159-164.

2. Berglund, L.A., Burgert, I. 2018. Bioinspired wood nanotechnology for functional materials. *Advanced Materials*, **30**(19), 1704285.

3. Coddington, J., Taylor, M. 1989. High Field11B and 13C Nmr Investigations of Aqueous Borate Solutions and Borate-Diol Complexes. *Journal of coordination chemistry*, **20**(1), 27-38.

4. Dai, L., Wang, Y., Liu, Y., Ruan, R., He, C., Yu, Z., Jiang, L., Zeng, Z., Tian, X. 2019. Integrated process of lignocellulosic biomass torrefaction and pyrolysis for upgrading bio-oil production: a state-of-the-art review. *Renewable and Sustainable Energy Reviews*, **107**, 20-36.

5. El Oudiani, A., Chaabouni, Y., Msahli, S., Sakli, F. 2011. Crystal transition from cellulose I to cellulose II in NaOH treated Agave americana L. fibre. *Carbohydrate Polymers*, **86**(3), 1221-1229.

6. Feng, N., Zheng, A., Wang, Q., Ren, P., Gao, X., Liu, S.-B., Shen, Z., Chen, T., Deng, F. 2011. Boron environments in B-doped and (B, N)-codoped TiO2 photocatalysts: a combined solid-state NMR and theoretical calculation study. *The Journal of Physical Chemistry C*, **115**(6), 2709-2719.

7. Haffner-Staton, E., Balahmar, N., Mokaya, R. 2016. High yield and high packing density porous carbon for unprecedented CO 2 capture from the first attempt at activation of air-carbonized biomass. *Journal of Materials Chemistry A*, **4**(34), 13324-13335.

8. He, X., Luzi, F., Yang, W., Xiao, Z., Torre, L., Xie, Y., Puglia, D. 2018. Citric acid as green modifier for tuned hydrophilicity of surface modified cellulose and lignin nanoparticles. *ACS Sustainable Chemistry & Engineering*, **6**(8), 9966-9978.

9. Herou, S., Ribadeneyra, M.C., Madhu, R., Araullo-Peters, V., Jensen, A., Schlee, P., Titirici, M. 2019. Ordered mesoporous carbons from lignin: a new class of biobased electrodes for supercapacitors. *Green chemistry*, **21**(3), 550-559.

10. Huber, G.W., Sara, I., Avelino, C. 2006. Synthesis of transportation fuels from biomass: chemistry, catalysts, and engineering. *Chemical Reviews*, **106**(9), 4044-4098.

11. Inari, G.N., Petrissans, M., Lambert, J., Ehrhardt, J., Gérardin, P. 2006. XPS characterization of wood chemical composition after heat-treatment. *Surface and Interface Analysis: An International Journal devoted to the development and application of techniques for the analysis of surfaces, interfaces and thin films*, **38**(10), 1336-1342.

12. Jayme, G. 1942. Preparation of holocellulose and cellulose with sodium chlorite. *Cellulosechemie*, **20**, 43-49.

13. Kartal, S.N., Hwang, W.-J., Imamura, Y. 2008. Combined effect of boron compounds and heat treatments on wood properties: Chemical and strength properties of wood. *Journal of Materials Processing Technology*, **198**(1-3), 234-240.

14. Kocaefe, D., Huang, X., Kocaefe, Y., Boluk, Y. 2013. Quantitative characterization of chemical degradation of heat-treated wood surfaces during artificial weathering using XPS. *Surface and Interface Analysis*, **45**(2), 639-649.

15. Kolpak, F.J., Blackwell, J. 1976. Determination of the Structure of Cellulose II. *Macromolecules*, **9**(2), 273-278.

16. Kosa, M., Ben, H., Theliander, H., Ragauskas, A.J. 2011. Pyrolysis oils from CO 2 precipitated Kraft lignin. *Green Chemistry*, **13**(11), 3196-3202.

17. Li, S., Lyons-Hart, J., Banyasz, J., Shafer, K. 2001. Real-time evolved gas analysis by FTIR method: an experimental study of cellulose pyrolysis. *Fuel*, **80**(12), 1809-1817.

18. Li, T., Liu, H., Zhao, X., Chen, G., Dai, J., Pastel, G., Jia, C., Chen, C., Hitz, E., Siddhartha, D. 2018a. Scalable and highly efficient mesoporous wood-based solar steam generation device: Localized heat, rapid water transport. *Advanced Functional Materials*, **28**(16), 1707134.

19. Li, T., Zhai, Y., He, S., Gan, W., Wei, Z., Heidarinejad, M., Dalgo, D., Mi, R., Zhao, X., Song, J., Dai, J., Chen, C., Aili, A., Vellore, A., Martini, A., Yang, R., Srebric, J., Yin, X., Hu, L. 2019. A radiative cooling structural material. *Science*, **364**(6442), 760-763.

20. Li, Y., Yang, X., Fu, Q., Rojas, R., Yan, M., Berglund, L. 2018b. Towards centimeter thick transparent wood through interface manipulation. *Journal of Materials Chemistry A*, **6**(3), 1094-1101.

21. Liu, W.-J., Jiang, H., Yu, H.-Q. 2015. Development of biochar-based functional materials: toward a sustainable platform carbon material. *Chemical Reviews*, **115**(22), 12251-12285.

22. Liu, Y., Li, G., Hu, Y., Wang, A., Lu, F., Zou, J.-J., Cong, Y., Li, N., Zhang, T. 2019. Integrated Conversion of Cellulose to High-Density Aviation Fuel. *Joule*, **3**(4), 1028-1036.

23. Lu, K., Hao, N., Meng, X., Luo, Z., Tuskan, G.A., Ragauskas, A.J. 2019. Investigating the correlation of biomass recalcitrance with pyrolysis oil using poplar as the feedstock. *Bioresource technology*, **289**, 121589.

24. Miyazaki, Y., Fujimori, T., Okita, H., Hirano, T., Yoshimura, K. 2013. Thermodynamics of complexation reactions of borate and phenylboronate with diol, triol and tetritol. *Dalton Transactions*, **42**(29), 10473-10486.

25. Patwardhan, P.R., Brown, R.C., Shanks, B.H. 2011. Product distribution from the fast pyrolysis of hemicellulose. *ChemSusChem*, **4**(5), 636-43.

26. Patwardhan, P.R., Satrio, J.A., Brown, R.C., Shanks, B.H. 2010. Influence of inorganic salts on the primary pyrolysis products of cellulose. *Bioresource technology*, **101**(12), 4646-4655.

27. Peng, Y., Liu, R., Cao, J. 2015. Characterization of surface chemistry and crystallization behavior of polypropylene composites reinforced with wood flour, cellulose, and lignin during accelerated weathering. *Applied Surface Science*, **332**, 253-259.

28. Peters, J.A. 2014. Interactions between boric acid derivatives and saccharides in aqueous media: Structures and stabilities of resulting esters. *Coordination Chemistry Reviews*, **268**, 1-22.

29. Ricardo, A., Carrigan, M., Olcott, A., Benner, S. 2004. Borate minerals stabilize ribose. *Science*, **303**(5655), 196-196.

30. Segal, L., Creely, J., Martin Jr, A., Conrad, C. 1959. An empirical method for estimating the degree of crystallinity of native cellulose using the X-ray diffractometer. *Textile research journal*, **29**(10), 786-794.

31. Shen, D., Gu, S., Bridgwater, A.V. 2010. Study on the pyrolytic behaviour of xylan-based hemicellulose using TG–FTIR and Py–GC–FTIR. *Journal of analytical and applied pyrolysis*, **87**(2), 199-206.

32. Shen, D.K., Gu, S. 2009. The mechanism for thermal decomposition of cellulose and its main products. *Bioresour Technol*, **100**(24), 6496-504.

33. Uner, I.H., Deveci, I., Baysal, E., Turkoglu, T., Toker, H., Peker, H. 2016. Thermal analysis of Oriental beech wood treated with some borates as fire retardants. *Maderas. Ciencia y tecnología*, **18**(2), 293-304.

34. Usman, M., Chen, H., Chen, K., Ren, S., Clark, J.H., Fan, J., Luo, G., Zhang, S. 2019. Characterization and utilization of aqueous products from hydrothermal conversion of biomass for bio-oil and hydro-char production: a review. *Green Chemistry*, **21**(7), 1553-1572.

35. Wang, H., Pu, Y., Ragauskas, A., Yang, B. 2019. From lignin to valuable products–strategies, challenges, and prospects. *Bioresource Technology*, **271**, 449-461.

36. Wang, Q., Li, J., Winandy, J. 2004. Chemical mechanism of fire retardance of boric acid on wood. *Wood Science and Technology*, **38**(5).

37. Wang, S., Jing, X., Wang, Y., Si, J. 2014. High char yield of aryl boron-containing phenolic resins: The effect of phenylboronic acid on the thermal stability and carbonization of phenolic resins. *Polymer Degradation and Stability*, **99**, 1-11.

38. Wang, S., Wang, Y., Bian, C., Zhong, Y., Jing, X. 2015. The thermal stability and pyrolysis mechanism of boron-containing phenolic resins: The effect of phenyl borates on the char formation. *Applied Surface Science*, **331**, 519-529.

39. Werner, K., Pommer, L., Broström, M. 2014. Thermal decomposition of hemicelluloses. *Journal of Analytical and Applied Pyrolysis*, **110**, 130-137.

40. Wicklein, B., Kocjan, D., Carosio, F., Camino, G., Bergström, L. 2016. Tuning the nanocellulose–borate interaction to achieve highly flame retardant hybrid materials. *Chemistry of Materials*, **28**(7), 1985-1989.

41. Xia, S., Gao, S., LI, J., Li, W. 1995. IR-spectra of borate. *Journal of Salt Lake Science*, **3**(3), 49-53.

42. Yu, F., Li, S., Chen, W., Wu, T., Peng, C. 2019. Biomass-Derived Materials for Electrochemical Energy Storage and Conversion: Overview and Perspectives. *Energy & Environmental Materials*, **2**(1), 55-67.

43. Zhang, K., Liu, M., Zhang, T., Min, X., Wang, Z., Chai, L., Shi, Y. 2019a. High-performance supercapacitor energy storage using a carbon material derived from lignin by bacterial activation before carbonization. *Journal of Materials Chemistry A*, **7**(47), 26838-26848.

44. Zhang, Z., Zhu, Z., Shen, B., Liu, L. 2019b. Insights into biochar and hydrochar production and applications: A review. *Energy*, **171**, 581-598.

Fig. 1. TGA curves of the tested lignocellulosic materials before and after boric acid treatment for, a) lignocellulose, b) holocellulose, c) MCC and d) lignin.

Fig. 2. TGA curves of polyols before and after boric acid treatment for, (a) glycerin and (b) mannitol, and DTG curves for (c) glycerin and (d) mannitol.

Fig. 3. Color parameters of the tested lignocellulose. (a) lightness (L^*), (b) redness (a^*), (c) yellowness (b^*), and (d) color difference (ΔE^*).

Fig. 4. The high resolution C1s spectra of pure lignocellulose and borated lignocellulose before and after heating. a) untreated lignocellulose, b) borated lignocellulose, c) lignocellulose treated by heating, and d) borated lignocellulose treated by heating.

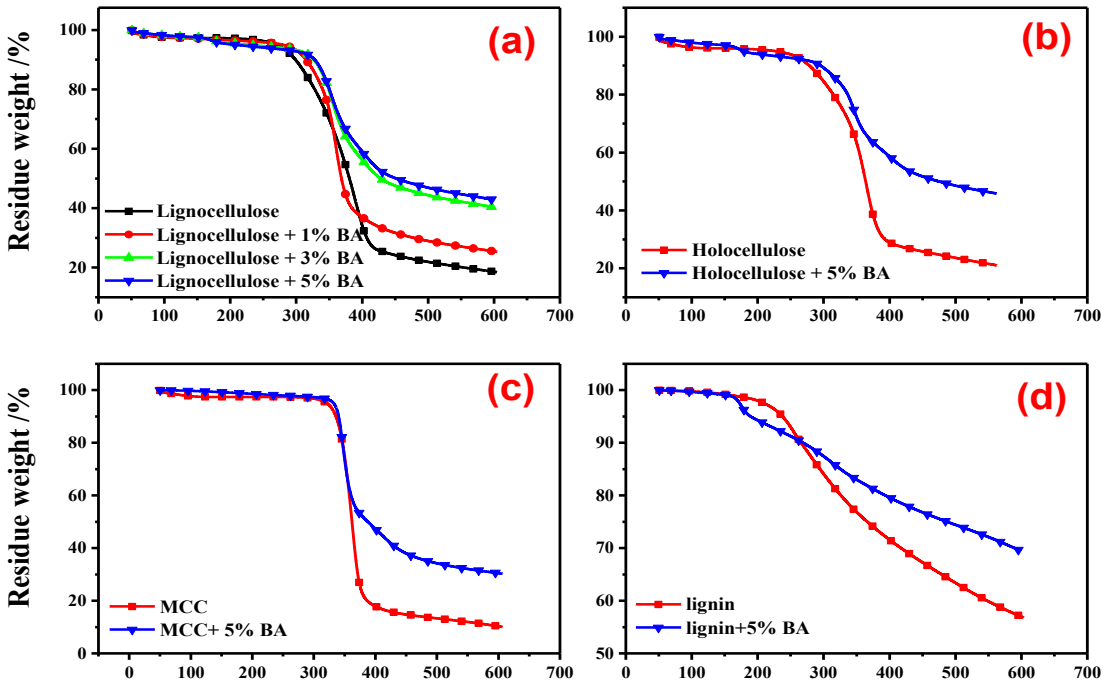

Fig. 1. TGA curves of the tested lignocellulosic materials before and after boric acid treatment for, (a) lignocellulose, (b) holocellulose, (c) MCC, d) lignin.

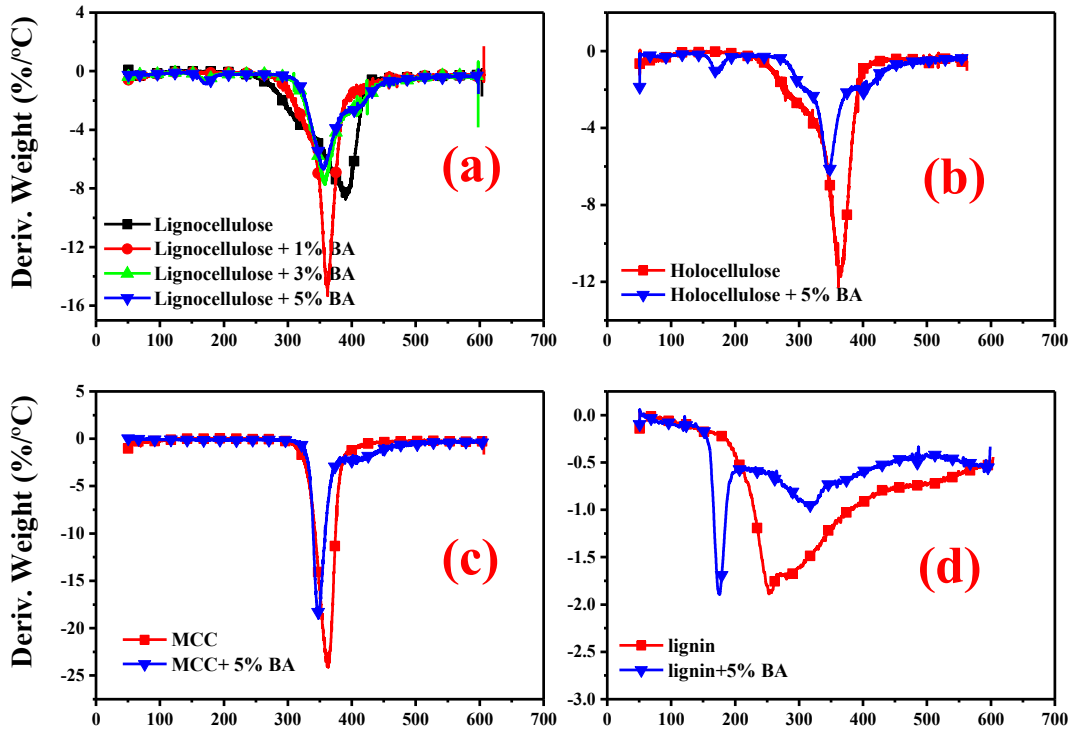

Fig. 2. DTG curves of the tested lignocellulosic materials before and after the boric acid treatment for, (a) lignocellulose, (b) holocellulose, (c) MCC, d) lignin.

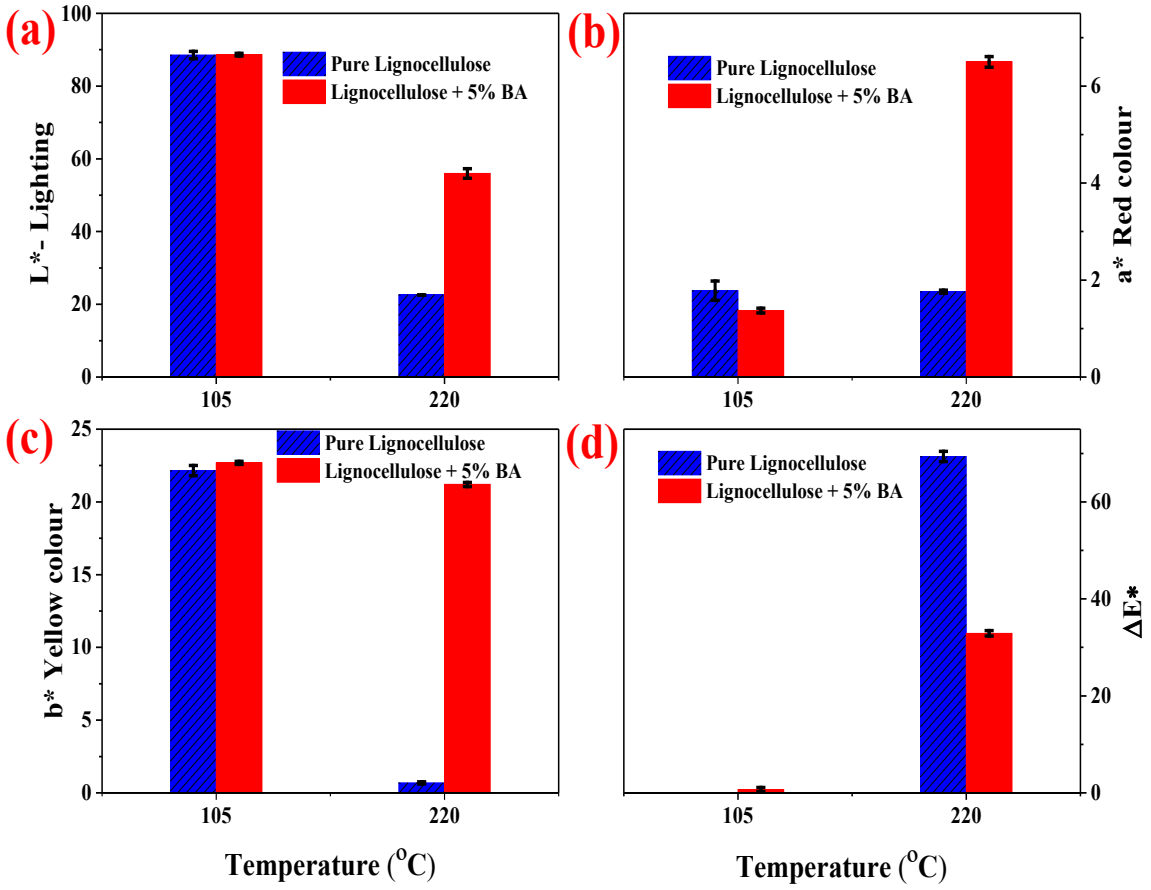

Fig. 3. Color parameters of the tested lignocellulose. (a) lightness (L^*), (b) redness (a^*), (c) yellowness (b^*), and (d) color difference (ΔE^*).

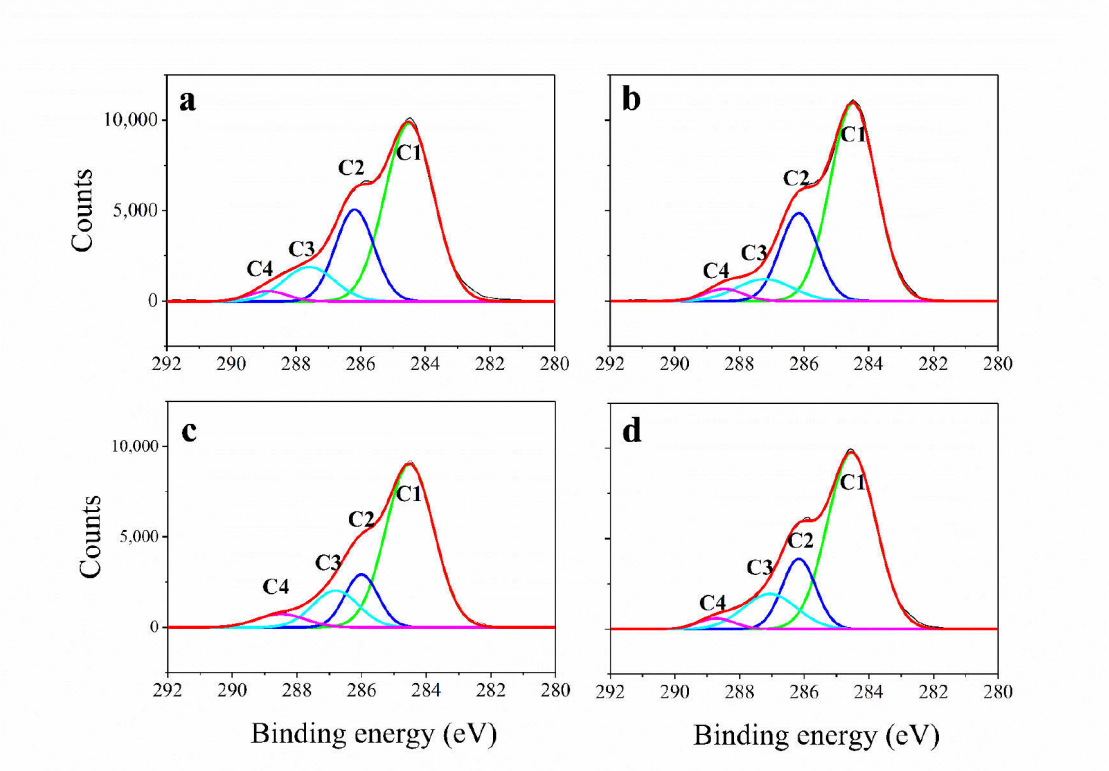

Fig. 4. The high resolution C1s spectra of pure lignocellulose and borated lignocellulose before and after heating. (a) untreated lignocellulose, (b) borated lignocellulose, (c) lignocellulose treated by heating, and (d) borated lignocellulose treated by heating.

Table 1. Summary of XPS spectral parameters of heat-treated lignocellulose

Samples	O/C	C_1%	C_2%	C_3%	C_4%
Lignocellulose	0.834	60.51	24.62	12.12	2.75
Lignocellulose + 5% BA	0.946	64.52	23.60	8.65	3.23
Heat treated lignocellulose	0.762	64.97	17.91	14.19	2.93
Heat treated lignocellulose+ 5% BA	0.948	65.76	14.73	14.12	5.39

Table 2. List of the main volatile compounds found among the products of lignocellulose and holocellulose identified by Py-GC/MS.

Number	Volatiles species	Molecular weight
1	Carbon dioxide	44
2	Methylglyoxal	72
3	Acetic acid	60
4	1-Hydroxy-2-acetone	74
5	Vinyl methyl ether	58
6	Methyl acetate	74
7	Furfural	96
8	1,2-Cyclopentanedione	98
9	Phenol	94
10	2-Methyl-phenol	108
11	2-methoxy-phenol	124
12	2-Methoxy-4-methyl-phenol	138
13	2,3-Dihydrofuran	70
14	2-Methoxy-4-vinylphenol	150
15	D-(-)-galactonic acid-γ-lactone	178
16	Phenol, 2,6-dimethoxy-	154
17	Phenol,2-methoxy-4-(1-propenyl)	164
18	Vanillin	152
19	Benzeneacetic acid, 4-hyroxy-3-methoxy-	182
20	Ethanone, 1-(4 hydroxy-3-methoxyphenyl)	166
21	4-methyl-3,5-dimethoxybenzaldehyde	180
22	4（5）-benzofuranone,6,7-dihydro-3,6-dimethyl-	164
23	Phenol, 2,6-dimethoxy-2-(2-propenyl)	194
24	Benzaldehyde,4-hydroxy-3,5-dimethoxy	182
25	4-hydroxy-3 methoxycinnamaldehyde	178
26	Unknow	-
27	Dibutyl phthalate	287
28	3,5-dimethoxy-4-hydroxycinnamaldehyde	208